Fluorescence

Deutsche Ausgabe: DOI: 10.1002/ange.201412107
Internationale Ausgabe: DOI: 10.1002/anie.201412107

The Design of Dual Emitting Cores for Green Thermally Activated Delayed Fluorescent Materials**

*Yong Joo Cho, Sang Kyu Jeon, Byung Doo Chin, Eunsun Yu, and Jun Yeob Lee**

Abstract: *Dual emitting cores for thermally activated delayed fluorescent (TADF) emitters were developed. Relative to the corresponding TADF emitter with a single emitting core the TADF emitter with a dual emitting core, 3,3′,5,5′-tetra(carbazol-9-yl)-[1,1′-biphenyl]-2,2′,6,6′-tetracarbonitrile, showed enhanced light absorption accompanied by a high photoluminescence quantum yield. The quantum and power efficiencies of the TADF devices were enhanced by the dual emitting cores.*

Thermally activated delayed fluorescent (TADF) devices have attracted great attention because both singlet and triplet excitons can be harvested for light emission by a reverse intersystem crossing process induced by a small singlet–triplet energy gap.[1–20] The small singlet–triplet energy gap is critical to the TADF emission of the emitter because the reverse intersystem crossing process can be activated by overcoming the energy barrier between singlet and triplet states. To realize a small singlet–triplet energy gap in the TADF emitter, the TADF emitter should be designed to reduce the singlet energy by separating the highest occupied molecular orbital (HOMO) and the lowest unoccupied molecular orbital (LUMO) using a donor–acceptor structure. Several TADF emitters have been developed based on the donor–acceptor molecular structure. (4s,6s)-2,4,5,6-tetra(9*H*-carbazol-9-yl) (4CzIPN) is one of the most well-known donor–acceptor-type TADF emitters with electron-donating carbazole and electron-withdrawing phthalonitrile moieties.[1] The HOMO and LUMO were separated by the donor–acceptor moieties and a small singlet–triplet energy gap of 0.12 eV was reported. Several derivatives of the phthalonitrile and carbazole moieties were synthesized and the number of nitrile (CN) and carbazole units was managed to change the emission spectrum of the TADF emitters. Other than this, several compounds derived from the donor–acceptor structure were developed and they had carbazole,[2–4] acridine,[5] triphenylamine,[6] and phenoxazine[7] moieties as the donor units, and sulfone,[2,5] ketone,[8] triazine[7] and dicyanofluorene[9] moieties as the acceptor units. These TADF emitters had a backbone structure with an electron-deficient core structure surrounded by electron-rich peripheral moieties or with an electron-deficient moiety directly connected with an electron-rich moiety. Although these materials exhibited TADF emission and an external quantum efficiency in the range of 10–20%, the molecular structure of the TADF emitters could not be diversified because the way of combining the donor and acceptor units is limited. Additionally, it is not known yet how to improve the quantum efficiency of the TADF devices by manipulating the molecular structure of the TADF emitters.

In this work, a novel TADF emitter design with a dual emitting core was reported and improved quantum efficiency by the dual core emitter design was demonstrated. A TADF emitter, 3,3′,5,5′-tetra(carbazol-9-yl)-[1,1′-biphenyl]-2,2′,6,6′-tetracarbonitrile (DDCzIPN), was synthesized by coupling two TADF emitter moieties and was characterized as the TADF emitter. A high quantum efficiency of 18.9% was achieved using the DDCzIPN TADF emitter and the quantum efficiency of the dual emitting core TADF emitter was enhanced compared to that of the single core TADF emitter with a single TADF emitter unit.

The novel dual core emitter design was devised based on the concept that light absorption is intensified by introducing multiple chromophores in the molecular structure of TADF emitters. The intensified light absorption would increase photoluminescence (PL) quantum yield of the TADF emitters and improve the quantum efficiency of the TADF devices. The basic concept of the dual core emitter design is described in Figure 1.

The dual core TADF emitter can be developed by simple coupling of two TADF emitters. A blue TADF emitter, 4,6-di(carbazol-9-yl)isophthalonitrile (DCzIPN),[20] can be coupled together by activating the central phenyl ring using lithium diisopropylamine (LDA) because the anion formed between two CN units by the LDA activation can be stabilized by two strong electron-withdrawing CN units. Hydroquinone-mediated coupling of two DCzIPN emitters produced DDCzIPN as the dual emitting core TADF emitter. The synthesis of DDCzIPN is shown in Scheme 1. The dual

[*] Y. J. Cho, Prof. B. D. Chin
Department of Polymer Science and Engineering
Dankook University
152, Jukjoen-ro, Suji-gu, Yongin, Gyeonggi, 448-701 (Korea)
S. K. Jeon, Prof. J. Y. Lee
School of Chemical Engineering, Sungkyunkwan University
2066, Seobu-ro, Jangan-gu, Suwon, Gyeonggi, 440-746 (Korea)
E-mail: leej17@skku.edu
Dr. E. Yu
Central R&D Center, Samsung SDI
Samsung-Ro 130, Yeongtong-Gu, Suwon, Gyeonggi-Do 443-803 (Korea)

[**] This work was supported by Samsung SDI, Basic Science Research Program through the National Research Foundation of Korea (NRF) funded by the Ministry of Education, Science and Technology (grant number 2013R1A1A2007991) and Ministry of Science, ICT and future Planning (grant number 2013R1A2A2A01067447) and development of red and blue OLEDs with external quantum efficiency over 20% using delayed fluorescent materials funded by MOTIE.

Supporting information for this article is available on the WWW under http://dx.doi.org/10.1002/anie.201412107.

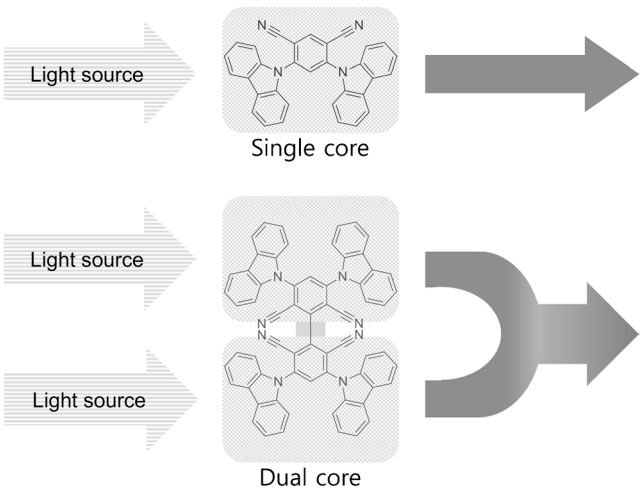

Figure 1. Basic concept of the dual emitting core design of TADF materials.

core TADF emitter was sublimed after purification by column chromatography to prepare highly pure final compounds. Chemical analysis using ^{1}H and ^{13}C nuclear magnetic resonance spectroscopy, mass spectrometry, and elemental analysis revealed that DDCzIPN was successfully synthesized by the coupling reaction. The purity of the compound was above 99%. Detailed chemical analysis data are given in the Supporting Information.

Light absorption and emission of the DDCzIPN were compared with those of DCzIPN to investigate the effect of coupling of the two TADF emitters. An ultraviolet–visible (UV/Vis) absorption spectrum, a spectrum of the solid PL in polystyrene, and a phosphorescence spectrum of DDCzIPN are displayed in Figure 2a. Corresponding UV/Vis and PL spectra of DCzIPN were added for comparison. As the basic concept of the dual emitting core design was to induce strong light absorption and accompanying intensified light emission by two chromophore moieties, absolution UV/Vis intensity was compared. The UV/Vis absorption of DDCzIPN was stronger than that of DCzIPN as anticipated and the absorption coefficient of DDCzIPN was increased from 1.1×10^{5} to $3.7\times10^{5}\,M^{-1}cm^{-1}$ by the absorption of the two TADF units. The intensified light absorption also enhanced the PL quantum yield of the TADF emitters and the increase of PL quantum yield from 0.67 to 0.91 was observed by the coupling of the two TADF units. In addition to the intense light absorption, the coupling of two TADF emitters shifted the UV/Vis and PL spectra to long wavelength because of the extension of conjugation caused by direct linkage between two phenyl units. The UV/Vis absorption edges of DCzIPN and DDCzIPN were 410 and 447 nm, respectively. The shift of the UV/Vis absorption edge of the TADF emitters by the coupling was 37 nm. A similar red-shift of the solid PL emission and phosphorescent emission by the coupling was also observed and PL peak positions of DCzIPN and DDCzIPN were 447 and 477 nm, respectively. The change of the PL emission by the coupling has its origin in the extended conjugation by the phenyl–phenyl coupling and strengthened donor–acceptor character by four carbazole and four CN units. Strong donor–acceptor character of the DDCzIPN molecule stabilized the charge-transfer singlet state and shifted the singlet PL emission of the TADF emitter. The triplet emission showed similar tendency to the singlet PL emission and the triplet energy was lowered by the direct coupling of the two TADF moieties. The singlet–triplet energy gap of DDCzIPN was 0.13 eV. The photophysical properties of DCzIPN and DDCzIPN emitters are compared in Table 1.

The molecular orbital distribution of the dual core TADF emitter was also explored and the HOMO and LUMO of the two emitters are displayed in Figure 2b. The HOMO dispersion on the carbazole unit and the LUMO localization on the CN-modified central phenyl ring were observed with weak overlap of the HOMO and LUMO on the central phenyl ring. DDCzIPN was found to have separated HOMO and LUMO for a small singlet–triplet energy gap and weakly overlapping HOMO and LUMO for efficient singlet emission. The HOMO and LUMO distribution of DDCzIPN was ideal for efficient delayed fluorescent emission.

The delayed emission and excited-state lifetime for the TADF emission were analyzed using transient PL measurements of the TADF emitters (Figure 2c). Delayed emission by the TADF emitters was observed and the lifetime for the delayed emission of DDCzIPN was 2.8 μs from numerical fitting of the PL decay curve. The lifetime of DDCzIPN was relatively short compared to that of other TADF emitters, which may be because of the rigidity of the molecular structure caused by steric hindrance of the four CN units in

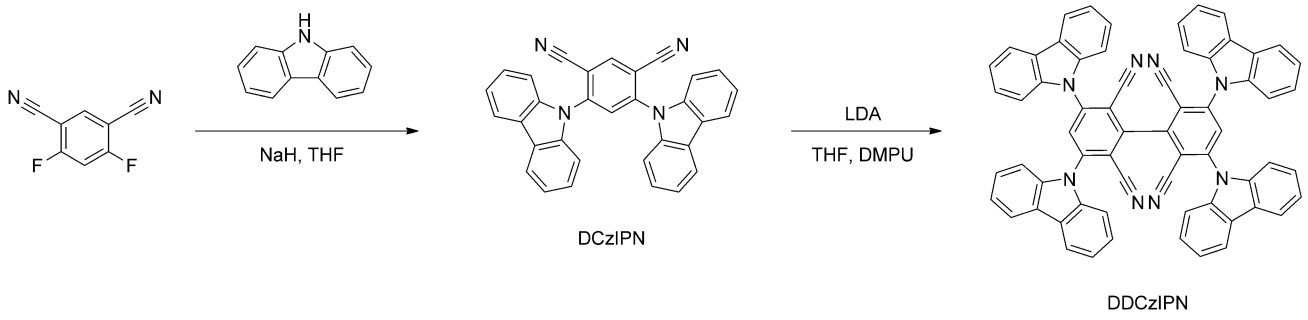

Scheme 1. Synthesis of DDCzIPN. LDA = Lithium diisopropylamide, THF = tetrahydrofuran, DMPU = 1,3-dimethyl-3,4,5,6-tetrahydro-2-pyrimidinone.

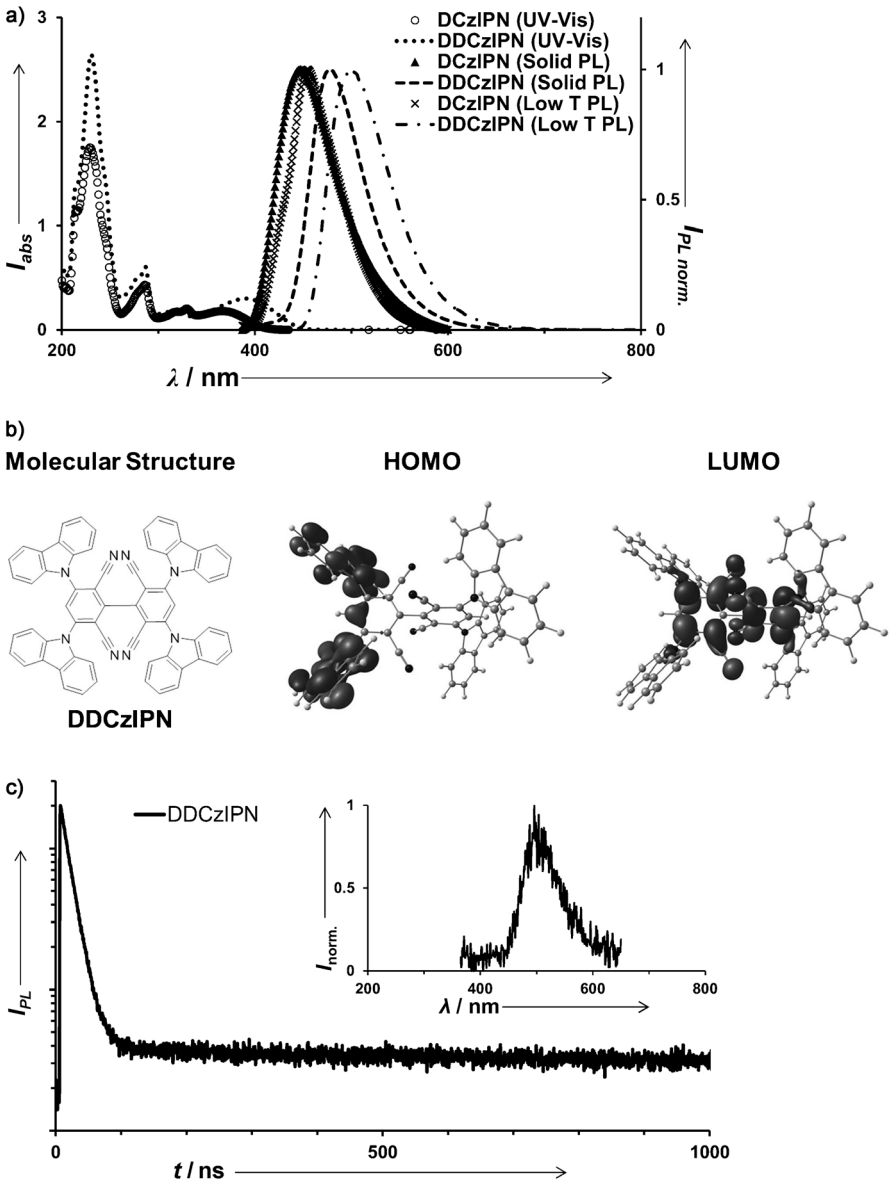

Figure 2. a) UV/Vis absorption and photoluminescence(PL) spectra of DCzIPN and DDCzIPN. UV/Vis absorption spectra were obtained from THF solution (concentrations 1.0×10^{-5} M). Solid PL spetra were obtained from polystryrene thin films with 1 wt% emitter coated on quartz. All data were collected at room temperature except for the low-temperature PL data at 77 K. b) The HOMO and LUMO and the molecular structure of DDCzIPN. Electron density distributions of the HOMO and LUMO were calculated by TD-DFT using Gaussian 09 software. c) PL decay curve of DDCzIPN in toluene (concentrations in the 10^{-5} M) with N_2 bubbling measured using a pulsed Nd-YAG laser (340 nm) as the excitation source and a photomultiplier tube as an optical detector system. The delayed PL emission spectrum of DDCzIPN is shown as an inset in this graph.

the central biphenyl moiety. A delayed PL emission spectrum of DDCzIPN was also added as an inset in Figure 2c, which was similar to the PL emission spectrum.

DDCzIPN was doped in the mixed host of 1,3-bis(*N*-carbazolyl)benzene (mCP) and 1,3,5-tri[(3-pyridyl)-phen-3-yl]benzene (BmPyPb) which was efficient as the host material for the green TADF dopant. The doping concentration of the TADF emitter was 1%. External quantum efficiency versus luminance graphs of the DDCzIPN devices are displayed in Figure 3a in addition to the quantum efficiency of the DCzIPN for comparison. The quantum efficiency of the dual emitting core TADF emitters was higher than that of the corresponding single emitting core TADF emitter. The maximum quantum efficiency of the DDCzIPN device was enhanced from 16.4% of the DCzIPN device to 18.9%. Strong light absorption and high PL quantum yield of the dual emitting core TADF emitter increased the quantum efficiency of the DDCzIPN device.

The electroluminescence (EL) spectrum of the DDCzIPN device was plotted in Figure 3b in comparison with that of the DCzIPN device. The EL spectra of the dual emitting core TADF emitters were red-shifted compared to those of the corresponding single emitting core TADF emitter, which agreed with the PL spectrum of the TADF emitters. The maximum emission peak of DDCzIPN was 497 nm, which corresponded to color coordinates of (0.22, 0.46). The device performances of the DDCzIPN device are summarized in Table 2 in addition to the device performances of DCzIPN.

Table 1: Photophysical properties of DCzIPN and DDCzIPN.

Compound	λ_{abs} [nm][a]	Φ_{PL} [%][b]	I_P/E_A [eV][c]	E_S/E_T [eV][d]	ΔE_{ST} [eV][e]	Calc. E_S/E_T [eV][f]
DCzIPN	222, 290, 332, 375	67	−6.40/−3.88	2.77/2.72	0.05	0.21
DDCzIPN	230, 287, 329, 400	91	−6.40/−3.88	2.60/2.47	0.13	0.15

[a] Measured in tetrahydrofuran solution (concentrations in the 10 μM range) at room temperature (RT). [b] Absolute PL quantum efficiency yield evaluated using an integrating sphere in toluene solution (concentrations in the 10 μM range). [c] Determined by using cyclic voltammetry analysis in the three-electrode mode with a carbon working electrode, a platinum wire counter electrode, and Ag/AgCl reference electrode. Nitrogen bubbling was conducted to remove oxygen from the sample before reduction measurement. [d] Singlet energy (E_S) estimated from peak wavelength of the 1 wt% doped film emission spectra in polystryrene on quartz at RT. Triplet energy (E_T) estimated from peak wavelength of tetrahydrofuran solution (concenctrations in the 10 μM range) emission spectra at 77 K. [e] $\Delta E_{ST} = E_S - E_T$. [f] Calculated by TD-DFT at B3LYP/6-31G(d).

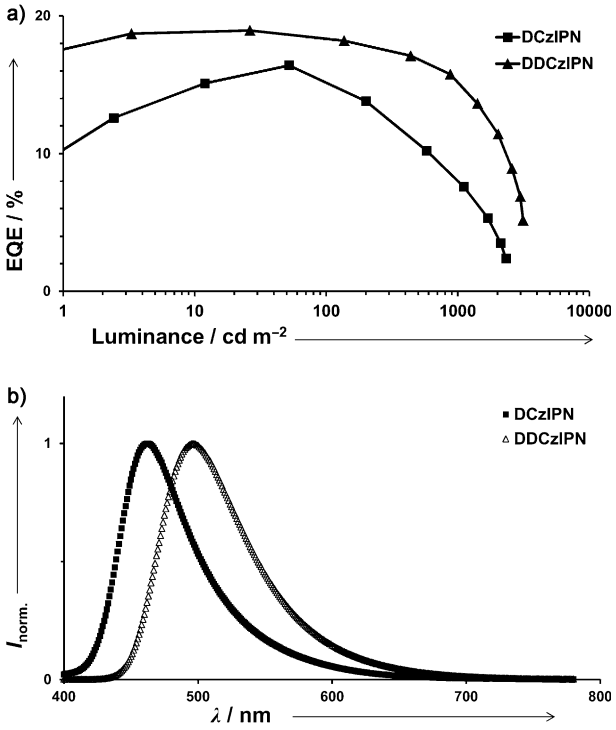

Figure 3. a) Plot of external quantum efficiency (EQE) versus luminance for DCzIPN and DDCzIPN devices. b) Plot of electroluminescent (EL) spectra for DCzIPN and DDCzIPN devices. The EL spectra were measured at 1000 cd m^{-2}.

Table 2: A summary of device performance of DCzIPN and DDCzIPN.

Emitter	Voltage[a]	CIE (x,y)[b]	Maximum EQE [%]	Maximum PE [Lm W^{-1}]	EQE [%][c]	PE [Lm W^{-1}][d]
DCzIPN	4.0	0.17, 0.19	16.4	15.9	7.6	4.8
DDCzIPN	3.5	0.22, 0.46	18.9	38.3	15.8	21.5

[a] Data of device turn on voltage. [b] Data of CIE 1931 color space measured at 1000 cd m^{-2}. [c] Data of external quantum efficiency (EQE) measured at 1000 cd m^{-2}. [d] Data of power efficiency (PE) measured at 1000 cd m^{-2}.

In conclusion, a dual emitting core TADF emitter, DDCzIPN, was synthesized as a novel high efficiency TADF emitter. The coupling of two TADF emitter moieties increased the quantum efficiency of the TADF device via enhanced absorption coefficient and PL quantum yield of the emitter. Therefore, the dual core TADF emitter design can be effectively used as the design strategy to improve the quantum efficiency of TADF emitters.

Experimental Section

Synthesis: Preparation methods of DDCzIPN are described in the Supporting Information in detail.

Device fabrication: The fabrication of the DDCzIPN device was conducted by stacking poly(3,4-ethylenedioxythiophene):poly(styrenesulfonate) (PEDOT:PSS), 4,4′-cyclohexylidenebis[*N*,*N*-bis(4-methylphenyl)aniline], mCP, mCP:BmPyPb:DDCzIPN, diphenylphosphine oxide-4-(triphenylsilyl)phenyl, 1,3,5-tris(*N*-phenylbenzimidazole-2-yl)benzene, LiF, and Al on an indium tin oxide (ITO) substrate. PEDOT:PSS was coated by a spin-coating process and other organic materials were deposited by vacuum thermal evaporation. Encapsulation of the devices was carried out by covering the ITO substrate with a glass lid.

Measurements: Chemical analysis of the synthesized materials is explained in the Supporting Information in detail. Transient PL measurement of the synthesized materials was performed using a pulsed Nd-YAG laser (340 nm) as the excitation source and a photomultiplier tube as an optical detector system. The absolute PL quantum efficiency value of the material (10 μM in Toluene) was determined using an integrating sphere at 340 nm excitation wavelength with N_2 bubbling.

Keywords: fluorescence · fluorescent materials · photochemistry · photoluminescence · quantum efficiency

How to cite: *Angew. Chem. Int. Ed.* **2015**, *54*, 5201–5204
Angew. Chem. **2015**, *127*, 5290–5293

[1] H. Uoyama, K. Goushi, K. Shizu, H. Nomura, C. Adachi, *Nature* **2012**, *492*, 236.
[2] F. B. Dias, K. N. Bourdakos, V. Jankus, K. C. Moss, K. T. Karntekar, V. Bhalla, J. Santos, M. R. Bryce, A. P. Monkman, *Adv. Mater.* **2013**, *25*, 3707.
[3] Y. J. Cho, K. S. Yook, J. Y. Lee, *Adv. Mater.* **2014**, *26*, 6642.
[4] Q. Zhang, J. Li, K. Shizu, S. Huang, S. Hirata, H. Miyazaki, C. Adachi, *J. Am. Chem. Soc.* **2012**, *134*, 14706.
[5] Q. Zhang, B. Li, S. Huang, H. Nomura, H. Tanaka, C. Adachi, *Nat. Photonics* **2014**, *8*, 326.
[6] H. Wang, L. Xie, Q. Peng, L. Meng, Y. Wang, Y. Yi, P. Wang, *Adv. Mater.* **2014**, *26*, 5198.
[7] H. Tanaka, K. Shizu, H. Miyazaki, C. Adachi, *Chem. Commun.* **2012**, *48*, 11392.
[8] S. Y. Lee, T. Yasuda, Y. S. Yang, Q. Zhang, C. Adachi, *Angew. Chem. Int. Ed.* **2014**, *53*, 6402; *Angew. Chem.* **2014**, *126*, 6520.
[9] G. Méhes, H. Nomura, Q. Zhang, T. Nakagawa, C. Adachi, *Angew. Chem. Int. Ed.* **2012**, *51*, 11311; *Angew. Chem.* **2012**, *124*, 11473.
[10] B. S. Kim, J. Y. Lee, *Adv. Funct. Mater.* **2014**, *24*, 3970.
[11] H. Nakanotani, K. Masui, J. Nishide, T. Shibata, C. Adachi, *Sci. Rep.* **2013**, *3*, 2127.
[12] Y. J. Cho, K. S. Yook, J. Y. Lee, *Adv. Mater.* **2014**, *26*, 4050.
[13] J. W. Sun, J. Lee, C. Moon, K. Kim, H. Shin, J. Kim, *Adv. Mater.* **2014**, *26*, 5684.
[14] C. Mayr, S. Y. Lee, T. D. Schmidt, T. Yasuda, C. Adachi, W. Bruttig, *Adv. Funct. Mater.* **2014**, *24*, 5232.
[15] B. S. Kim, K. S. Yook, J. Y. Lee, *Sci. Rep.* **2014**, *4*, 6019.
[16] D. Zhang, L. Duan, C. Li, Y. Li, H. Li, D. Zhang, Y. Qiu, *Adv. Mater.* **2014**, *26*, 5050.
[17] B. S. Kim, J. Y. Lee, *ACS Appl. Mater. Interfaces* **2014**, *6*, 8396.
[18] Y. Im, J. Y. Lee, *Chem. Mater.* **2014**, *26*, 1413.
[19] V. Jankus, P. Data, D. Graves, C. McGuinness, J. Santos, M. R. Bryce, F. B. Dias, A. P. Monkman, *Adv. Funct. Mater.* **2014**, *24*, 6178.
[20] Y. J. Cho, K. S. Yook, J. Y. Lee, *Sci. Rep.* **2014**, *5*, 7859.

Received: December 18, 2014
Published online: February 26, 2015

